Removing Orbital-dependence to Improve Exchange-Correlation Functional Accuracy

H. Francisco,*,† A.C. Cancio,‡ and S.B. Trickey*,¶

†*Quantum Theory Project, Dept. of Physics, University of Florida, Gainesville FL 32611, USA*
‡*Dept. of Physics and Astronomy, Ball State University, Muncie IN 47306, USA*
¶*Quantum Theory Project, Dept. of Physics and Dept. of Chemistry, University of Florida, Gainesville FL 32611, USA*

E-mail: francisco.hector@ufl.edu; trickey@ufl.edu

Dated: 11 July 2025

Abstract

De-orbitalization (replacement of orbital dependence by an explicit density functional) of a meta-generalized gradient approximation for exchange and correlation has been deemed successful if the de-orbitalized functional delivers simple error bounds comparable to those from the parent functional on standard data sets. Tacitly it has been assumed that de-orbitalization will not improve on those errors. One counter-example is known, at least on molecular data sets, the meta-GGA made very simple (MVS) functional; see *Phys. Rev. A* **2017**, *96*, 052512. On the basis of post-SCF calculations [*J. Chem. Phys.* **2018**, *149*, 144105], it was argued that the unexpected betterment on molecules provided by that one specific de-orbitalizer does not occur in solids. Some other de-orbitalizers considered in that later work did show performance betterment of MVS on solids however. But molecules were not treated nor was the issue of ambiguous betterment pursued. We revisit the issue and show that the betterment of MVS for that particular de-orbitalizer does occur in solids when the calculations are done self-consistently and with the same computational techniques as used in other de-orbitalizations. For systems without d states or without transition metals, that betterment is improved. Imposition of second-order gradient expansion compliance as a constraint upon the de-orbitalizer refines (rather than degrades) the improvement relative to the parent MVS functional and provides insight as to why de-orbitalized MVS behaves differently from other de-orbitalized meta-GGA functionals.

Motivation

Discussion and use of the Perdew-Schmidt "Jacob's ladder" complexity hierarchy[1] for approximate exchange-correlation (XC) density functionals typically involves the expectation that adding specific functional variables will improve accuracy and applicability. Thus, at the third rung of the ladder, most meta-generalized-gradient approximations (meta-GGAs) add the Kohn-Sham kinetic energy density,

$$\tau_s[\{\varphi\}] = \frac{1}{2}\sum_i f_i |\nabla\varphi_i(\mathbf{r})|^2 \tag{1}$$

with f_i and φ_i the occupation numbers and Kohn-Sham (or generalized KS; see below) orbitals respectively, to the electron number density $n(\mathbf{r})$ and its dimensionless reduced gradient

$$s := \frac{|\nabla n(\mathbf{r})|}{2(3\pi^2)^{1/3} n^{4/3}(\mathbf{r})} \tag{2}$$

used in GGAs. Examples include TPSS,[2,3] revTPSS,[4] SCAN,[5,6] Tao-Mo,[7–9] and r^{2}SCAN.[10]

The primary question addressed here is this: can the performance of such a meta-GGA be improved by de-orbitalization, that is, replacement of the τ_s orbital dependence with $\nabla^2 n$ dependence instead? Tacitly (and anecdotally), the common view of the numerical evidence amongst functional developers seems to be that the answer is negative. However there is some mixed and thus far unpursued evidence to the contrary, as we summarize below. The main result of this work is to provide an unequivocal example of an affirmative answer to the question. We also investigate the causes and show that re-imposition of constraints yields a superior betterment.

The context is this. Inclusion of τ_s in the suite of functional variables enables straightforward use of chemical-region-indicator functions, e.g. the well-known[11]

$$\alpha[\{\varphi\}] := \frac{\tau_s - \tau_W}{\tau_{TF}} \tag{3}$$

with

$$\begin{aligned} \tau_{TF} &:= \frac{3}{10}(3\pi^2)^{\frac{2}{3}}\, n^{5/3}(\mathbf{r}) \equiv c_{TF}\, n^{5/3}(\mathbf{r}) && (4)\\ \tau_W &:= \frac{1}{8}\frac{|\nabla n(\mathbf{r})|^2}{n(\mathbf{r})}\ , && (5)\end{aligned}$$

the Thomas-Fermi and von Weizsäcker kinetic energy densities respectively. Being able to detect chemically distinct regions should give meta-GGAs substantially greater accuracy and broader applicability than GGAs.

Two related limitations arise from utilizing τ_s. Although in principle the optimized effective potential procedure[12–14] could be used to obtain a proper (*i.e.*, local) Kohn-Sham XC potential, OEP is computationally costly. Thus it is common practice to use the generalized Kohn-Sham procedure instead. That gives, for example, an orbital-dependent X potential $v_x[\varphi_i] = \delta E_x^{mGGA}/\delta\varphi_i$. Ordinary KS and generalized-KS are the same for pure (i.e. orbital-independent) functionals but not for explicitly orbital-dependent ones.[15]

The related limitation is that, depending on computational implementation and system complexity, generalized-KS can be anywhere from 30% to more than a 100% slower than KS. For high-throughput searches such an increment can be prohibitive; see discussion in Ref. 16.

De-orbitalization of a meta-GGA XC functional replaces the τ_s orbital dependence with an approximate pure density functional. Typically the dependence is limited to n, ∇n, and $\nabla^2 n$ for reasons of numerical tractability. After a couple of early de-orbitalization examples,[17,18] Mejía-Rodríguez and Trickey[19–21] devised and applied a protocol denoted hereafter as "M-RT". For functionals with τ_s dependence only through α (the plainest case), the M-RT approach is to select, from the orbital-free kinetic energy density functional (KEDF) literature,[22] some promising approximate KEDFs, $\tau_s[n, \{\phi\}] \approx \tau[n, \nabla n, \nabla^2 n]$. Each candidate then is reparametrized to give a good approximation to the orbital-dependent α,

$$\alpha_L[n, \nabla n, \nabla^2 n] \approx \alpha[\{\varphi\}] \tag{6}$$

rather than the original KEDF objective of producing a good approximation to $T_s[n]$, the KS kinetic energy. (Henceforth, the subscript "L" denotes density-Laplacian dependence.) Alteration of a known functional form of a candidate de-orbitalizer also is possible of course.

A de-orbitalizer form of particular interest here is Cancio-Redd[23]

$$\alpha_{\mathrm{CR}} := 1 + z\Theta_{\mathrm{CR}}(z)\ . \tag{7}$$

Here z is from the second-order gradient expansion

$$z := \frac{20}{9}q - \frac{40}{27}p\ , \tag{8}$$

with the dimensionless reduced density Laplacian

$$q := \frac{\nabla^2 n}{4(3\pi^2)^{2/3} n^{5/3}}\ , \tag{9}$$

and switching function

$$\Theta_{\mathrm{CR}}(z) = \left[1 - \exp\left(-\frac{1}{|z|^A}\right)(1 - H(z))\right]^{1/A}\ . \tag{10}$$

$H(z)$ is the Heaviside unit step function and

$A = 4$. The M-RT reparametrization, denoted CRopt, is

$$z_{opt} := aq + bp \tag{11}$$

with $a = -.295491$, $b = 2.615740$.

M-RT deemed a de-orbitalization to be satisfactory and called it "faithful" if it delivered simple error bounds (mostly mean absolute deviations, MADs) with respect to standard molecular and crystalline data sets that matched the error bounds from the parent functional closely. For molecules, those data sets are the G3X/99 223 test set for molecular heats of formation (computed according to the procedure of Curtiss *et al.*[24,25]), the T96-R test set[26,27] for optimized bond lengths, and the T82-F test set[26,27] for harmonic vibrational frequencies. For solids, the test sets for static lattice constants and cohesive energies include 55 systems,[28] while for bulk moduli there are 44 systems.[29] Band gaps of 21 insulators and semiconductors[30] were used to test Kohn-Sham (KS) and generalized-KS (g-KS) bands.

There was a surprise in the original M-RT work.[19] Table 1 reproduces the key molecular results. [Note that the value tabulated in Ref. 19 for the CRopt heat of formation MAD, 6.20 kcal/mol, is incorrect, the result of a transcription error. The correct value, 7.83 kcal/mol is shown.[31]] De-orbitalization of the MVS (meta-GGA made very simple) functional[32] with the CRopt KEDF mentioned above gave a heat of formation MAD substantially smaller (about a factor of 2.3) than the MAD from the parent functional. The bond length MAD was slightly smaller and the frequency MAD 18% smaller. M-RT called this unexpected improvement over the parent functional a *best-performance* de-orbitalization.[19] That is in contrast with the *faithful* results for the PCopt de-orbitalization (though the PCopt MADs are modestly better than for the parent). PCopt is M-RT's reparametrization of the Perdew-Constantin KED.[18]

Though MVS-L(CRopt) is substantially better, at least on molecules, as a pure meta-GGA than its conventional orbital-dependent τ_s-based parent, that oddity has gone largely ignored with respect to solids. Almost all solid-system exploration and testing of the M-RT approach, Refs. 8,20,21,33, omitted MVS-L. The one exception is a study by Tran et al.[34] From post-SCF all-electron calculations with densities from the PBE GGA,[35] they concluded that the MVS-L(CRopt) best-performance molecular outcome does not occur in solids. It worsens the $E_{cohesive}$ MAD slightly in their calculations, for example. They, in fact, characterized the seemingly close resemblance of MVS-L(CRopt) behavior to parent functional behavior as "fortuitous" because the mean errors of the parent and de-orbitalized functionals are "completely different and of opposite sign." Intriguingly, however, they also noticed that some other de-orbitalizers of MVS decreased MADs versus the parent. They attributed that sensitivity to the strong dependence of the MVS functional upon de-orbitalizer form. They did not pursue the issue.

Thus there is a question left hanging from Refs. 19 and 34: Does CRopt provide a best-performance de-orbitalization of MVS for both molecules and solids? Answering that amounts to determining whether the negative outcome reported in Ref. 34 is, in fact, intrinsic to MVS-L(CRopt) or is a consequence of procedure (post-SCF evaluation on PBE densities). The diverse and essentially unexplored other findings from Ref. 34 also motivate the investigation of other de-orbitalizers of MVS: are there others that provide best-performance-level results?

Tests of MVS-L(CRopt) on solids and molecules

Methods

With the exception of Ref. 34, to our knowledge all of the testing of the M-RT strategy has been with NWChem for molecules and VASP for solids.[9,19–21,33,36]

For thoroughness of comparisons (including any possible software version issues), we redid the molecular tests of MVS-L(CRopt) on the G3X/99, T-96R, and T-82F data sets with NWChem[37] version 7.0.2, Def2-TZVPP basis

Table 1: Comparison of molecular test set results for best-performance (CRopt) and faithful (PCopt) de-orbitalized versions of the MVS XC functional as reported in Ref. 19 (with corrected CRopt heat of formation MAD.[31]) Heat of formation errors in kcal/mol, bond length errors in Å, frequency errors in cm^{-1}. ME = mean error, MAE = mean absolute error.

	Error	CRopt	PCopt	MVS parent
Heats of formation	ME	2.89	-15.37	-17.33
	MAD	7.83	15.94	18.34
Bonds	ME	0.0049	-0.0025	-0.0016
	MAD	0.0130	0.0127	0.0139
Frequencies	ME	28.7	39.3	46.2
	MAD	42.6	46.0	52.0

sets,[38] and `xfine` grid settings.

To assess effects related to the implementation of periodic boundary conditions (e.g. plane wave cutoffs, etc.), we also did counterpart quasi-isolated molecule calculations with VASP[39] version 5.4.4. Those calculations employed a very large orthorhombic cell, with the molecule positioned at the center, and at least 10 Å of vacuum from a cell boundary to the outermost atom of the molecule. The default energy cutoff was overridden and set to 600 eV for all molecular systems. The precision parameter was set to `accurate` (PREC=A), and the conjugate gradient minimization algorithm (ALGO=A) was used. Non-spherical contributions within the PAW spheres were included self-consistently (LASPH=.TRUE.). Also, Gaussian-type thermal smearing with width = 0.01 eV was used. First Brillouin zone integrations were restricted to the Γ point.

For the quasi-isolated molecule calculations with VASP, the charged species members of the T96-R set had to be omitted. The result is a 46-molecule subset to determine the bond length, denoted here by T-46R. For it, we followed the same methodological choices as for the G3X/99 calculations, except that we used a threshold of 2×10^{-3} eV/Å for the forces (EDIFFG = -0.002).

One motive for comparing isolated molecule calculations from VASP against those from NWChem is that projector augmented wave (PAW) data sets for meta-GGAs are unavailable in VASP. We used PBE[35] PAWs as is common, widespread practice and as was done in the previous M-RT studies. Note that harmonic frequencies for isolated molecules are not readily available from VASP, so we report only the NWChem results for those.

For the periodic solids we also used VASP. The methodological choices for those calculations were close to those for the quasi-isolated molecules. However, the energy cutoff was set to 800 eV, and Brillouin zone integrations used 17 × 17 × 17 Γ-centered symmetry-reduced Monkhorst-Pack[40] k-meshes and the tetrahedron method with Blöchl corrections.[41] For hexagonal close-packed structures, the ideal c/a ratio was used. For cohesive energies, the isolated-atom energies were done in a 14 × 15 × 16 Å unit cell and Γ point Brillouin zone sampling.

For purposes of comparison and checking, we also re-did the data-set studies for the r^{2}SCAN and r^{2}SCAN-L meta-GGA functionals, thus both extending the previous study of MVS-L to solids as well as rechecking the coding and calculations of Ref. 19 for molecules on MVS and MVS-L and of Ref. 21 for r^{2}SCAN and r^{2}SCAN-L.

Numerical results

Tables 2, 3, and 4 compile mean errors (ME) and MADs for MVS, MVS-L(PCopt), MVS-L(CRopt), MVS-L(CR), r^{2}SCAN, and r^{2}SCAN-L (with the PCopt de-orbitalizer, the best found by M-RT). Those three tables also provide results from PBE[35] as a baseline. The r^{2}SCAN-L results provide an example of what tacitly is taken to be typical: only a "faithful" de-orbitalization has been found.

First we answer the motivating question: Is CRopt a best-performance de-orbitalization of MVS for both molecules and crystals? In that regard, MAD comparison may seem a rather minimal measure on which to base comparisons of XC functionals, in the context of "faithful" versus "best-performance" de-orbitalizations. But that comparison provides an unequivocal distinction. High-performing and poorly-performing de-orbitalizations are unambiguously identifiable from MAD comparisons alone. As is clear from those three Tables, that is the case with diverse de-orbitalizers of MVS.

Though the tabulated results do show some periodic-system effects (from VASP; Table 3) in the isolated molecule tests, those effects do not change the earlier key finding. The "best performance" de-orbitalization of MVS from CRopt found previously in molecules[19] is reproduced (Tables 2 and 3) *irrespective of the computational methodology.* The molecular heat of formation MAD for MVS-L(CRopt) is reduced by a factor of 2.3 in *both* the NWChem and VASP calculations. In stark contrast, de-orbitalization of r^{2}SCAN *increases* the heat of formation MAD by 18% in the NWChem calculations and by a factor of 2.14 in the VASP calculations.

Moreover, that best-performance distinction is unequivocally present in solids (Table 4). MVS-L(CRopt) MADs are notably better than the parent functional MADs for cohesive energies (16 % reduction for CRopt) and lattice parameters (24% reduction), and 33% better on bulk moduli. Consistent with the molecular pattern, CRopt is a distinctly better de-orbitalizer than PCopt. Note again the contrast with the de-orbitalization of r^{2}SCAN to r^{2}SCAN-L(PCopt). In that de-orbitalization the a_0 MAD worsens slightly, the E_{coh} MAD worsens by 45%, and the B_0 MAD worsens by 73%.

In both the molecular and solid cases therefore there is a qualitative difference between de-orbitalizations of MVS and of r^{2}SCAN. For MVS, there is a de-orbitalization benefit, while for r^{2}SCAN there is a de-orbitalization penalty. (Note that the band-gap penalty for de-orbitalization is about the same from MVS to MVS-L(CRopt) as from r^{2}SCAN to r^{2}SCAN-L. Basically this is a measure of the difference between g-KS and KS.)

In short, the original best-performance finding of Ref. 19 regarding CRopt is upheld. The contrary result of Ref. 34 thus provokes additional investigation.

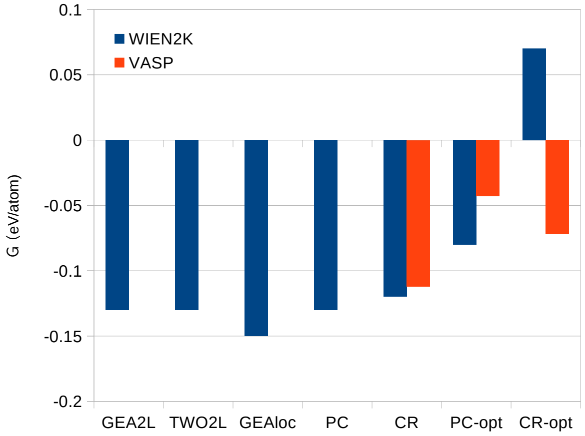

Figure 1: De-orbitalization shift $\mathfrak{G}$ in cohesive energy MAD relative to parent XC functional MAD for 7 de-orbitalizations of MVS. Blue data are from Ref. 34, orange are present work. Units are eV/atom.

Motivation for such investigation is reinforced by the somewhat obliquely discussed findings of Ref. 34 regarding six other de-orbitalizers. Distinct from their results for MVS(CRopt), Ref. 34 reports notable de-orbitalization betterment from all six. We confirmed this finding by repeating our VASP calculations with two de-orbitalizers that share commonality with CRopt. They are CR, which shares the same functional form, albeit with different parameters, and PCopt, which shares an origin in the MR-T methodology of fitting parameters to reproduce the KED of small atoms. What both our calculations and those of Ref. 34 demonstrate is that their MVS-L(CRopt) results for solids are an outlier. A simple way to show that is to compare the de-orbitalization-induced

Table 2: Molecular results (recalculated with NWChem) of the MVS and MVS-L XC functionals using the CRopt and CR de-orbitalizers with comparisons for r^{2}SCAN, r^{2}SCAN-L (with PCopt de-orbitalizer), and PBE XC functionals. Heat of formation errors in kcal/mol, bond length errors in Å, and frequency errors in cm^{-1}.

		MVS	MVS-L(CRopt)	MVS-L(CR)	r^{2}SCAN	r^{2}SCAN-L	PBE
Heats of formation	ME	-17.226	3.012	-2.933	-3.145	1.845	-20.878
	MAD	18.242	7.845	6.906	4.488	5.300	21.385
Bond distances (T96-R)	ME	-0.002	0.005	0.005	0.005	0.008	0.018
	MAD	0.014	0.013	0.012	0.010	0.011	0.018
Frequencies	ME	47.24	28.58	5.607	11.34	-7.25	-33.78
	MAD	51.44	42.46	28.240	30.90	25.71	43.61

Table 3: Molecular results as in Table 2 but from VASP calculations and with bond lengths for T-46R; see text.

		MVS	MVS-L(CRopt)	r^{2}SCAN	r^{2}SCAN-L	PBE
Heats of formation	ME	-16.845	-5.745	0.870	6.194	-18.020
	MAD	17.864	7.675	3.671	7.881	18.693
Bond distances T46-R	ME	0.001	0.007	0.008	0.006	0.016
	MAD	0.013	0.014	0.010	0.012	0.016

Table 4: Comparison of errors for XC combinations for four solid test sets. Equilibrium lattice constant errors in Å, cohesive energy errors in eV/atom, bulk modulus errors in GPa, and Kohn-Sham (and g-KS) band gap errors in eV.

		MVS	MVS-L (PCopt)	MVS-L (CRopt)	MVS-L (CR)	r^{2}SCAN	r^{2}SCAN-L	PBE
Lattice Constants	ME	-0.015	-0.024	0.024	-0.019	0.026	0.022	0.046
	MAD	0.045	0.039	0.034	0.032	0.037	0.039	0.053
Cohesive energies	ME	0.292	0.026	-0.236	0.270	-0.134	-0.331	-0.070
	MAD	0.457	0.414	0.385	0.345	0.238	0.346	0.252
Bulk moduli	ME	16.012	13.027	0.647	8.582	1.367	-4.008	-9.704
	MAD	16.695	18.935	11.143	12.262	5.963	10.345	11.022
Band Gaps	ME	-0.76	-1.162	-1.11	-1.43	-1.20	-1.38	-1.69
	MAD	1.12	1.30	1.24	1.46	1.20	1.38	1.69

shift in $E_{cohesive}$, defined as

$$\mathfrak{S}_{cohesive} := MAD^{deorb}_{cohesive} - MAD^{parent}_{cohesive} \,. \quad (12)$$

A de-orbitalization betterment has $\mathfrak{S}_{cohesive} < 0$. Fig. 1 displays the comparison.

Somewhat surprisingly, the best performing de-orbitalizer is CR, not only for solids but for molecules: see Table 2. CR has the property of satisfying the second-order gradient expansion for the kinetic energy. Its use instead of CRopt therefore restores the second-order gradient expansion compliance lost with CRopt. That such restoration improves molecular as well as solid performance is the somewhat surprising aspect. We return to that finding in the detailed analysis of constraints and slowly-varying limits presented below.

Beyond these major outcomes, some technical aspects need to be addressed. For the isolated molecules, the primary causes of the difference between NWChem and VASP results in Tables 2 and 3 surely are finite-size effects (large periodic box rather than vacuum boundary conditions) and the aforementioned use of PBE PAW data sets. Both are in contrast with the consistent all-electron treatment in NWChem. Note also that in the comparison of the heat of formation and cohesive energy results, the physical systems are quite different. The G3X/99 set consists predominantly of light to medium inorganic and organic molecules while the crystalline data set is dominated by elemental solids with a few diatomics. We will return to that distinction below as a means of diagnosis of de-orbitalization efficacy.

Importantly, however, none of those differences obscures the main finding. Plainly there is a best-performance de-orbitalization of MVS (in fact, two) for *both molecules and solids*.

Given the contrast of these MVS-L(CRopt) results with those of Ref. 34, it is important to consider procedural differences. Among the most obvious is post-SCF effects. Table 5 provides that comparison. Both the WIEN2K calculations in Ref. 34 and our post-SCF VASP calculations used self-consistent densities and orbitals from the PBE exchange-correlation functional.[35] Their calculations were explicitly all-electron, ours with PBE PAWs as described already. The $\mathrm{E}_{cohesive}$ reference dataset they used is a 44-system subset of the 55-system data set we ordinarily use. Our post-SCF results in Table 5 are for that smaller set, which is why the values differ from those in Table 4.

Tran et al. found that MVS-L(CRopt)@PBE gave worse MADs than MVS for $\mathrm{E}_{cohesive}$ (0.44 vs. 0.37 eV/atom) or lattice constants a_0 (0.050 vs. 0.043 Å), but better MAD for bulk moduli B_0 (10.1 vs. 13.3 GPa). Our post-SCF evaluation has the MADs for both $\mathrm{E}_{cohesive}$ and a_0 essentially the same for MVS-L(CRopt)@PBE vs. MVS@PBE (0.394 vs. 0.409 eV/atom; 0.046 vs. 0.047 Å).

The key point is that these post-SCF data differ qualitatively from the self-consistent results. Unlike the post-SCF outcomes, *none* of the self-consistent results (aside from band gap, which implicates a gKS versus KS aspect) shows a substantial MAD increase upon de-orbitalization of MVS with CRopt. Regarding that SCF versus post-SCF difference, Table 5 shows that $\mathrm{E}_{cohesive}$ from MVS-L(CRopt) is sensitive to the difference between its own self-consistent density and the PBE density whereas the τ_s-dependent parent functional, MVS, is not. It is quite plausible, at the least, that this density-Laplacian sensitivity is the primary cause of the inconsistency of the post-SCF results with the self-consistent ones. The post-SCF results (both ours and those of Ref. 34) clearly are erroneous in indicating that the CRopt de-orbitalization of MVS does not provide a best-performance result for solids.

As an aside, one of our original reasons for reconsidering MVS was to seek insight into the over-magnetization of *3d* elemental solids exhibited by the more sophisticated SCAN functional, which also uses only the α indicator. See Ref. 42 and references therein. Our results for that ancillary investigation are in the Supporting Information.

Simple analysis

To investigate the betterment of MVS by MVS-L(CRopt), first we examine the fidelity of a de-orbitalized α to its orbital-dependent par-

Table 5: Comparison of our solid-system post-SCF results (MADs), denoted "@PBE", and those from Ref. 34 in brackets, along with our self-consistent VASP results for MVS and MVS-L(CRopt). See text regarding cohesive energy data set.

Solid	MVS@PBE	MVS-L(CRopt)@PBE	MVS	MVS-L(CRopt)	PBE
$E_{cohesive}$ (eV/atom)	0.409	0.394	0.407	0.327	0.349
	[0.37]	[0.44]			
a_0 (Å)	0.046	0.047	0.051	0.035	0.060
	[0.043]	[0.050]			
B_0 (GPa)	15.23	9.04	16.70	11.14	11.82
	[13.3]	[10.1]			

ent. Fig. 2 compares α versus α_L, for MVS and MVS-L(CRopt), respectively, for four molecules, Na_2, Ar_2, BeH, and C_3H_4 (propyne). The first two exemplify metallic and overlap binding. BeH is an open-shell diatomic molecule with simple bonding. C_3H_4 is a more complex organic molecule with multiple atoms and several types of bonds and functional groups. The four molecules thus facilitate rapid assessment of molecular bonding effects. For all four, the α_L indicator mirrors α closely except for large distances from the molecule. This local correctness clearly contributes to the successful de-orbitalization. But it gives little insight into the best-performance aspect.

Fig. 3 therefore shows the difference between α and α_L for two choices of de-orbitalizer, CRopt and PCopt. Recall that PCopt gave the "faithful" de-orbitalization. For both de-orbitalizers, it is apparent that the most significant difference typically occurs in regions distant from the nuclei, whereas in the vicinity of the nuclei, the difference typically is much less, albeit slightly increasing in the bonding region for the tested molecules.

Generally PCopt is inferior to CRopt. Comparison of $\Delta\alpha_L$(CRopt) and $\Delta\alpha_L$(PCopt) shows that the PCopt de-orbitalizer typically has small to moderately greater error with respect to the orbital α. Particularly in Na_2, in the outer bonding region $\Delta\alpha_L$(PCopt) underestimates more than $\Delta\alpha_L$(CRopt). This suggests that α_L(PCopt) overestimates the orbital α by more than twice the amount of α_L(CRopt). In the bonding region, particularly for Ar_2, the PCopt error in the region between the two closed-shell Ar atoms is spectacular. The very large α seen is typical of exponential tails in the density, which one might expect for a non-covalent bond (also seen in BeH, but without the large de-orbitalization error).

Regarding the original question, whether a best-performance de-orbitalization exists (or was only a special case for molecules), the incorrect post-SCF result (recall Table 5 and discussion) make it seem plausible, at least at first thought, that the MVS-L(CRopt) and PBE densities are substantially different. But density plots revealed little difference to the eye. The evidence in that Table instead is strongly suggestive of a density-driven shift. MVS-L(CRopt) seems to be more sensitive to density than MVS. As mentioned above, plausibly that sensitivity comes from the density Laplacian dependence of MVS-L

Earlier we noted that the G3X/99 set consists predominantly of light to medium inorganic and organic molecules while the 55 solid data set is dominated by elemental solids with a few diatomic systems. The distinction leads to considering how the crystalline results would change if materials with *d*-states were removed. That can be tested in at least two ways, by removing all the systems with *d*-states or by removing the systems with transition metal constituents. Table 6 shows both outcomes in self-explanatory fashion. Either way, MVS-L(CRopt) yields better lattice constant results than even r^2SCAN. For systems with no *d*-states, the MVS-L(CRopt) cohesive energy MAD is better than for r^2SCAN-L and close to competitive with r^2SCAN (which im-

Table 6: Comparison of results for the full 55 crystal test set, for a subset with no transition metals, and another subset of 18 solids with lighter elements without *d* states [C, Si, SiC, BN, BP, AlN, AlP, LiH, LiF, LiCl, NaF, NaCl, MgO, Li, Na, K, Ca, and Al].

		Lattice constants (Å):			
		MVS	MVS-L(CRopt)	r^2SCAN	r^2SCAN-L
55 solid test set	ME	-0.015	0.024	0.026	0.022
	MAD	0.045	0.034	0.037	0.039
No Transition metals	ME	-0.011	0.017	0.041	0.027
	MAD	0.060	0.028	0.051	0.047
No *d* states	ME	-0.041	0.006	0.013	-0.006
	MAD	0.050	0.021	0.029	0.028
		Cohesive energies (eV/atom):			
		MVS	MVS-L(CRopt)	r^2SCAN	r^2SCAN-L
55 solid test set	ME	0.292	-0.236	-0.134	-0.331
	MAD	0.457	0.385	0.238	0.346
No Transition metals	ME	0.275	0.071	-0.031	-0.141
	MAD	0.309	0.117	0.078	0.149
No *d* states	ME	0.246	0.061	-0.022	-0.105
	MAD	0.295	0.109	0.074	0.119
		Bulk modulus (Gpa):			
		MVS	MVS-L(CRopt)	r^2SCAN	r^2SCAN-L
44 solids	ME	16.012	0.647	1.367	-4.008
	MAD	16.695	11.143	5.963	10.345
No Transition metals	ME	10.207	1.928	-0.442	-3.135
	MAD	10.862	5.676	3.288	5.464
No *d* states	ME	10.082	1.458	0.068	-2.418
	MAD	10.861	7.270	4.466	6.283

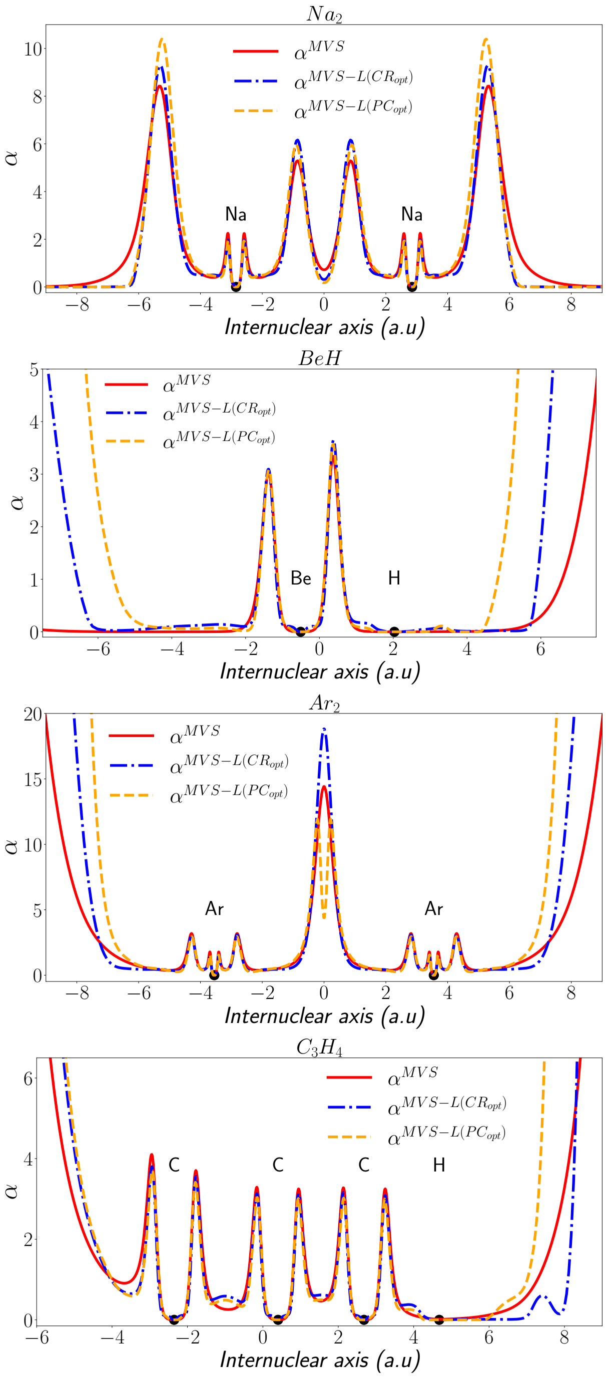

Figure 2: Orbital-dependent α and its de-orbitalized approximation for four different molecules, Na_2, BeH, Ar_2 and C_3H_4 (propyne) using MVS and MVS-L(CRopt) XC functionals. Each is evaluated self-consistently with the XC functional as labeled. Solid dots indicate nuclear positions.

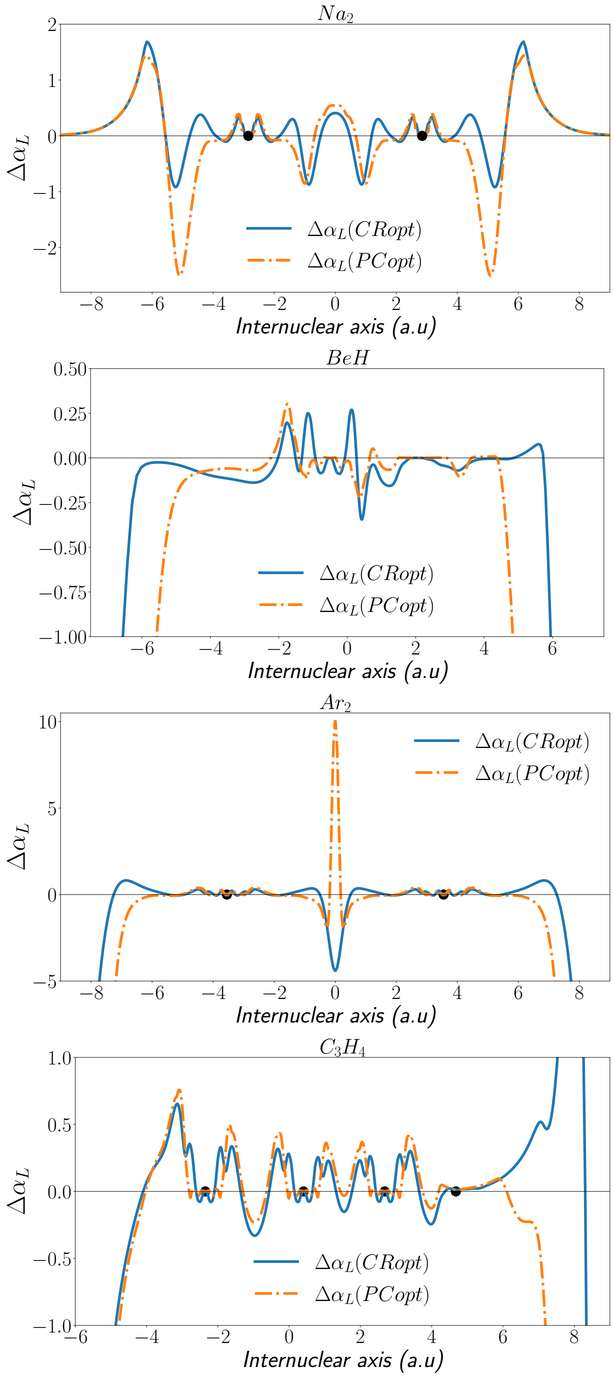

Figure 3: Difference of $\alpha^{MVS} - \alpha^{MVS-L}$ denoted as $\Delta\alpha_L$ for both de-orbitalizers CRopt and PCopt for the same molecules as in Fig. 2.

plicates a much more demanding calculation).

This behavior suggests that a limitation of MVS, and hence of its de-orbitalized versions, is that it does not handle the spurious self-repulsion (that is particularly strong for *d*-states) as well as somewhat more sophisticated meta-GGAs such as r^{2}SCAN. It seems relevant that MVS was made very simple by removing much of the meta-GGA functionality meant for approximate treatment of, among other things, self-interaction error. We note also that CRopt was parametrized to fit *low-Z* atoms which have no *d* states, a difference that may also be implicated in its limitations in this regard.

Constraints and slowly-varying limit

We mentioned already that there was a bit of a surprise in Tables 2 and 4, namely that the Cancio-Redd ("CR")[23] de-orbitalizer works as well or better than CRopt. MVS-L(CR) is an improvement not only over MVS but also over MVS-L(CRopt). The CR heat of formation MAD improves over the CRopt value by 12%. The CR versus CRopt E_{cohesive} MAD improvement for molecular frequencies is dramatic (33%), while the bond length and lattice parameter improvements are slight. The bulk modulus MAD is a little worse. Overall this makes MVS-L(CR) almost competitive with the far more complicated r^{2}SCAN-L and better-balanced between molecules and solids than PBE.

Careful, retrospective study of the Supplemental Material Tables for Ref. 34 makes this realization less surprising. Those authors found three de-orbitalizers of MVS that reduced the solid-system MADs by roughly 60% compared to the MVS parent. All three are closely related to the second-order gradient expansion for KE.

A related clue is in the reduction in heat of formation MAD in going from CRopt to CR de-orbitalization of MVS. That contrasts with the situation with PBEsol.[43] It is a modification of the PBE exchange that restores the exact second-order gradient expansion for exchange in the slowly varying limit, namely $\mu_{\text{eff}} = 10/81$ (see below). That modification leads, in general, to improvements in solid structural parameter errors at the expense of some reduction in accuracy of calculated cohesive energies and molecular heats of formation.

The metric M-RT used to select candidate de-orbitalizers[19] caused them to miss the improvement from CR over CRopt. They did recognize that their approach can break constraints that are respected in the parent τ_s-dependent functional, for example, the second-order gradient expansion but did not pursue that issue. In the one instance known to us in which constraint compliance for de-orbitalization has been tried thoroughly, it gave disappointing performance[33] in the sense of a bias to metallic systems.

The present numerical results (as well as some of those from Ref. 34) suggest, strongly, that the situation with MVS is different. In MVS, α, Eq. (3), defines almost all the behavior of the exchange enhancement function. The exception is a modification that is relevant only at large values of s^2. Thus, unlike other α-based meta-GGAs such as SCAN,[5,6] constraint noncompliance in a model α_L can have large effects upon the resulting MVS-L.

The PCopt α_L violates both the homogeneous electron gas (HEG) limit ($s = 0$) and the second-order gradient expansion for the KED of the slowly-varying gas. MVS-L(PCopt) exchange is incorrect for both of those important limits therefore. This noncompliance is a byproduct of prioritizing the production of realistic molecular test set binding energies (via fitting of α to atomic kinetic energies) without hurting predictions for solids significantly.

Recognition of the noncompliance provides insight into plausible cause for why M-RT found the PCopt de-orbitalizer to be effective only in the sense of their "faithful" de-orbitalization;[19] recall discussion above. In the same vein, changing from PCopt to CRopt, M-RT's "best-performance" de-orbitalizer,[19] restores the HEG limit. But the resulting de-orbitalization still deviates from the second-order gradient expansion.

The simple structure of MVS enables a correspondingly simple gradient expansion analysis, as follows. For weakly inhomogeneous densities, the CR expression for α is

$$\alpha = 1 + as^2 + bq - a_W s^2 \equiv 1 + z \tag{13}$$

with $a_W = 5/3$ and a, b values dependent on the parametrization. With $a = 5/27$, $b = 20/9$, CR is just the second-order gradient expansion. Ref. 32 showed that in MVS the q-dependent term can be expressed solely in terms of s (by an integral by parts) as

$$z = -(a + b/3 - a_W)s^2 \ . \tag{14}$$

For the weakly inhomogeneous case, $\alpha \approx 1$, hence $|z|$ is small and it follows rather easily that the MVS X enhancement factor becomes

$$\begin{aligned} F_x &\approx 1 + \kappa_x z \ , \\ \kappa_x &:= \frac{k_0}{\left[(1+e_1)^2 + c_1\right]^{1/4}} \ . \end{aligned} \tag{15}$$

The constants k_0 and e_1 are determined by other considerations in the MVS construction, leaving c_1 to determine κ_x and hence compliance or non-compliance with the gradient expansion with z as in Eq. (14). To get the canonical value requires

$$\frac{20}{27}\kappa_x = \mu_{GE} \equiv \frac{10}{81}, \tag{16}$$

which requires $\kappa_x = 1/6$.

Reparametrization, however, changes a and b, so with $\kappa_x = 1/6$ fixed we have

$$F_x \approx 1 + \mu_{\text{eff}} s^2 \tag{17}$$

with

$$\mu_{\text{eff}} := -\frac{1}{6}(a + b/3 - a_W) \ . \tag{18}$$

In contrast to CR (with the GE value $\mu_{\text{eff}} = \mu_{\text{GE}} = 10/81 \approx 0.12345679$), CRopt has $a = -0.29541$, $b = 2.615740$,[19] which gives $\mu_{\text{CRopt}} = 0.1817$, a 47% increase.

Now recall that PBE[35] has $\mu_{\text{eff}} = 0.2194$, substantially farther from the second-order gradient expansion value than μ_{CRopt}. PBEsol,[43] by comparison has μ_{GE}. A consequence is that PBE is more successful on molecules than PBEsol and conversely for solids. An obvious question for MVS de-orbitalization is this: Does preservation of the gradient expansion limit in exchange via use of CR better solid-property MADs at the expense of losing predictive power for finite systems? Our findings, in Tables 2 and 4, show the contrary, a pleasant surprise. Both molecular energetics and crystalline cohesive energies are improved by gradient expansion compliance, i.e., going from CRopt to CR.

In this context, it also is instructive to recall that the MVS correlation energy is a modification of the PBE form.[35] The modification is of the density gradient coefficient, denoted β in PBE, from its high-density value (in PBE), 0.0066725, to an approximate representation of its correct density-dependent form,[44]

$$\beta(r_s) = 0.066725 \frac{1 + 0.1 r_s}{1 + 0.1778 r_s} \tag{19}$$

with $r_s = (3/4\pi)^{1/3} n^{-1/3}$, the Wigner-Seitz radius. The design choice made in using Eq. (19) is to have the second-order gradient contributions from exchange and correlation cancel in the high-density limit ($r_s \to 0$).[44]

Because the CRopt de-orbitalizer modifies the second-order gradient expansion, it negates that cancellation. Use of the CR functional restores it. The result with CR therefore is consistent satisfaction to second-order in gradient expansions. It seems highly plausible that this is the reason for the unexpected success of CR as a de-orbitalizer of MVS.

Timing

A continuing challenge to the de-orbitalization strategy is the numerical difficulties that often are introduced by $\nabla^2 n$ dependence. MVS-L(CRopt) is an example. Table 7 presents the number of SCF cycles and the timings calculated for the six molecule test set AE6[45] and a test set of six solids. The crystalline phases used were the diamond structure for C, Si, Ge, and Sn, and the zincblende structure for SiC and BN. Experimental lattice constants (C 3.553 Å, Si 5.421 Å, Ge 5.644 Å, Sn 6.477 Å, SiC 4.346 Å, BN 4.592 Å) were employed for the calculations with both functionals.

The AE6 calculations were performed using NWChem-7.0.2, following the methodology outlined in Methods (above). Correspondingly, the calculations for the six solids were conducted using the VASP code, also as described above. The calculations were performed on a machine with an AMD EPYC 75F3 32-core processor. For the molecular calculations, 8 cores and 4GB of memory per core were allocated, while for the solid calculations, all 32 cores were utilized, each with the same memory allocation. The computations were executed in parallel.

For the AE6 molecular test set, the table shows that MVS-L(CRopt) requires slightly more SCF cycles than MVS to converge for each molecule, Since the time per cycle is substantially longer, the total time taken for all molecules more than doubles for MVS-L(CRopt) compared to MVS. This involves a 21.4 % increase in the number of SCF cycles for MVS-L relative to MVS.

Different behavior is observed for the solid test set, In two of the six cases (C, BN), the total time is lower for MVS-L(CRopt) than for the parent functional. For the other four systems, MVS is faster overall. The difference clearly is a consequence of the fact that for all six solids the number of SCF cycles needed by MVS-L(CRopt) is substantially larger than with MVS. Of course, the de-orbitalized functional provides a time advantage only if the time per SCF cycle is sufficiently lower than that of the parent functional to offset the need for more cycles. Such an accelerated SCF cycle time is consistent with the expected advantage of going from g-KS to pure KS. Nonetheless, the presence of $\nabla^2 n$ dependence in the de-orbitalized functional causes so much slower iteration-to-iteration SCF convergence that the cycle time advantage is lost. In the particular case of Table 7, MVS-L(CRopt) needs approximately 42.9 % more time than MVS because of needing over three times the number of SCF cycles.

Concluding remarks

The best-performance de-orbitalization of MVS (CRopt) found in Ref. 19 for molecules also outperforms the parent meta-GGA functional on crystalline cohesive energy, though the improvement is not as big. The previous finding to the contrary about cohesive energy[34] apparently was a result of post-SCF evaluation and the effects of using PBE orbitals in the orbital-dependent parent functional. An even better example of best-performance de-orbitalization of MVS, MVS-L(CR) was discovered in this study. It illustrates the significance of compliance with gradient expansion behavior for weakly inhomogeneous regions. MVS-L(CR) is almost competitive with the far more sophisticated de-orbitalized meta-GGA r^{2}SCAN-L for molecular and crystalline energetics. Therefore, it may be of some practical use for early iterations in calculations on complicated, costly systems. It also remains interesting as a provocation for seeking other best-performance de-orbitalizations.

The reason that MVS differs from r^{2}SCAN in its de-orbitalization behavior may be the fundamental difference in the structure of the two functionals. MVS exchange is built almost entirely on the single parameter α alone, (hence the “made very simple" moniker). In MVS α is used to (i) describe the second-order gradient expansion for the slowly-varying electron gas, (ii) produce a self-interaction-free exchange energy for the single-orbital limit, and (iii) provide a switching function based on its capacity for in bond-identification. Only a modest change due to the variable s^2 at very large values of s is used in MVS. More intricate (and more numerically accurate) meta-GGAs use α in a somewhat more limited way. SCAN, in particular, uses it mainly as a bond-region indicator and as a minor correction to enforce fourth-order gradient expansion in the slowly-varying limit. r^{2}SCAN does essentially the same except for the fourth-order gradient expansion.

The penalty for the strong structural dependence of MVS upon α seems to be its unusually large cohesive energy and heat of formation errors. Replacing $\alpha(\{\phi\})$ with an explicit functional of the density moves the de-orbitalized form to something quite similar to other de-orbitalized forms (resembling a modified GGA). A related aspect of this dependence seems to

Table 7: Total timings, number of SCF cycles and times per SCF cycle calculated for each molecule of the molecular test set AE6 and for a test set of six solids. The AE6 calculations were done with NWChem code whereas the solid calculations were done with VASP.

Molecules		MVS	MVS-L(CRopt)	Solids		MVS	MVS-L(CRopt)
SiH_4	Total time (s)	2.1	4.9	C	Total time (s)	33.1	30.8
	Total cycles	5	6		Total cycles	12	22
	Time/cycle	0.42	0.82		Time/cycle	2.76	1.40
SiO	Total time (s)	1.5	4.2	Si	Total time (s)	84.3	157.9
	Total cycles	9	10		Total cycles	16	105
	Time/cycle	0.17	0.42		Time/cycle	5.27	1.50
S_2	Total time (s)	2.1	4.2	Ge	Total time (s)	102.4	155.4
	Total cycles	7	8		Total cycles	15	80
	Time/cycle	0.30	0.53		Time/cycle	6.82	1.94
C_3H_4 (propyne)	Total time (s)	8.7	24.8	Sn	Total time (s)	122.3	179.1
	Total cycles	7	12		Total cycles	15	82
	Time/cycle	1.24	2.07		Time/cycle	8.15	2.18
$C_2H_2O_2$ (glyoxal)	Total time (s)	8.0	12.4	SiC	Total time (s)	50.5	62.0
	Total cycles	8	8		Total cycles	15	49
	Time/cycle	1.00	1.55		Time/cycle	3.37	1.27
C_4H_8 (cyclobutane)	Total time (s)	23.6	42.0	BN	Total time (s)	41.2	34.7
	Total cycles	6	7		Total cycles	16	26
	Time/cycle	3.93	6.00		Time/cycle	2.58	1.33
Overall	Total time (s)	46.0	92.5	Overall	Total time (s)	433.8	619.9
	Total cycles	42	51		Total cycles	89	364

be that sacrificing the second-order gradient approximation in a de-orbitalized α for a more accurate description of the first 18 neutral atoms (the parametrization scheme) is not an effective way to gain realism for bonded systems. This is in contrast to the case for meta-GGAs with more muted dependence on α. Instead, preserving the second-order gradient expansion through use of the CR de-orbitalizer produces a somewhat better de-orbitalization improvement over MVS. At the least, it is quite plausible that a functional in which α plays a quite dominant role should be more affected by de-orbitalization than a more complicated meta-GGA. The numerical results presented here are consistent with that appraisal. MVS-L(CRopt) also exposes the importance of finding computationally better ways of formulating and handling $\nabla^2 n$ dependence.

Supporting Information Available

The Supporting Information is available free of charge as MVS_revisited.SuppInfo In this file we provide

- Results of magnetization for MVS, MVS-L versus PBE for bcc Fe, hcp Co, and fcc ni
- detailed, system-by-system tabulation of the numerical results of the test calculations against standard molecular and solids.
- A brief discussion of self-consistent parametrization of CRopt.

Acknowledgement We thank Dr. Angel Albavera Mata for a helpful remark about MVS correlation. Work supported by U.S. National Science Foundation grant DMR-1912618.

References

(1) Perdew, J. P.; Schmidt, K. Jacob's ladder of density functional approximations for the exchange-correlation energy. AIP Conf. Proc. **2001**, 577, 1–20.

(2) Tao, J.; Perdew, J. P.; Staroverov, V. N.; Scuseria, G. E. Climbing the Density Functional Ladder: Nonempirical Meta–Generalized Gradient Approximation Designed for Molecules and Solids. Phys. Rev. Lett. **2003**, 91, 146401.

(3) Perdew, J. P.; Tao, J.; Staroverov, V. N.; Scuseria, G. E. Meta-generalized gradient approximation: Explanation of a realistic nonempirical density functional. J. Chem. Phys. **2004**, 120, 6898–6911.

(4) Ruzsinszky, A.; Sun, J.; Xiao, B.; Csonka, G. I. A meta-GGA Made Free of the Order of Limits Anomaly. J. Chem. Th. Comput. **2012**, 8, 2078–2087.

(5) Sun, J.; Ruzsinszky, A.; Perdew, J. P. Strongly Constrained and Appropriately Normed Semilocal Density Functional. Phys. Rev. Lett. **2015**, 115, 036402.

(6) Sun, J.; Remsing, R. C.; Zhang, Y.; Sun, Z.; Ruzsinszky, A.; Peng, H.; Yang, Z.; Paul, A.; Waghmare, U.; Wu, X. et al. Accurate first-principles structures and energies of diversely bonded systems from an efficient density functional. Nat. Chem. **2016**, 8, 831–836.

(7) Jana, S.; Behera, S. K.; Śmiga, S.; Constantin, L. A.; Samal, P. Accurate density functional made more versatile. J. Chem. Phys. **2021**, 155, 024103.

(8) Francisco, H.; Cancio, A. C.; Trickey, S. B. Reworking the Tao–Mo exchange-correlation functional. I. Reconsideration and simplification. J. Chem. Phys. **2023**, 159, 214102.

(9) Francisco, H.; Cancio, A. C.; Trickey, S. B. Reworking the Tao–Mo exchange–correlation functional. II. De-orbitalization. J. Chem. Phys. **2023**, 159, 214103.

(10) Furness, J. W.; Kaplan, A. D.; Ning, J.; Perdew, J. P.; Sun, J. Accurate and Numerically Efficient r^{2}SCAN Meta-Generalized Gradient Approximation. J. Phys. Chem. Lett. **2020**, 11, 8208–8215.

(11) Sun, J.; Xiao, B.; Fang, Y.; Haunschild, R.; Hao, P.; Ruzsinszky, A.; Csonka, G. I.; Scuseria, G. E.; Perdew, J. P. Density Functionals that Recognize Covalent, Metallic, and Weak Bonds. Phys. Rev. Lett. **2013**, 111, 106401.

(12) Städele, M.; Majewski, J. A.; Vogl, P.; Görling, A. Exact Kohn-Sham Exchange Potential in Semiconductors. Phys. Rev. Lett. **1997**, 79, 2089–2092.

(13) Grabo, T.; Kreibich, T.; Gross, E. K. U. Optimized Effective Potential for Atoms and Molecules. Mol. Eng. **1997**, 7, 27–50.

(14) Grabo, T.; Kreibach, T.; Kurth, S.; Gross, E. K. U. In Strong Coulomb Correlations in Electronic Structure: Beyond the Local Density Approximation; Anisimov, V. I., Ed.; Gordon and Breach: Tokyo, 2000; p 203, (refs. therein).

(15) Heßelmann, A.; Görling, A. Comparison between optimized effective potential and Kohn–Sham methods. Chemical Physics Letters **2008**, 455, 110–119.

(16) Teale, A. M.; Helgaker, T.; Savin, A.; Adamo, C.; Aradi, B.; Arbuznikov, A. V.; Ayers, P. W.; Baerends, E. J.; Barone, V.; Calaminici, P. et al. DFT exchange: sharing perspectives on the workhorse of quantum chemistry and materials science. Phys. Chem. Chem. Phys. **2022**, 24, 28700–28781.

(17) Lee, C.; Yang, W.; Parr, R. G. Development of the Colle-Salvetti correlation-energy formula into a functional of the

electron density. Phys. Rev. B **1988**, 37, 785–789.

(18) Perdew, J. P.; Constantin, L. A. Laplacian-level density functionals for the kinetic energy density and exchange-correlation energy. Phys. Rev. B **2007**, 75, 155109.

(19) Mejía-Rodríguez, D.; Trickey, S. B. Deorbitalization strategies for meta-generalized-gradient-approximation exchange-correlation functionals. Phys. Rev. A **2017**, 96, 052512.

(20) Mejía-Rodríguez, D.; Trickey, S. B. Deorbitalized meta-GGA exchange-correlation functionals in solids. Phys. Rev. B **2018**, 98, 115161.

(21) Mejía-Rodríguez, D.; Trickey, S. B. Meta-GGA performance in solids at almost GGA cost. Phys. Rev. B **2020**, 102, 121109.

(22) Mi, W.; Luo, K.; Trickey, S. B.; Pavanello, M. Orbital-Free Density Functional Theory: An Attractive Electronic Structure Method for Large-Scale First-Principles Simulations. Chem. Rev. **2023**, 123, 12039–12104.

(23) Cancio, A. C.; Redd, J. J. Visualisation and orbital-free parametrisation of the large-Z scaling of the kinetic energy density of atoms. Mol. Phys. **2017**, 115, 618–635.

(24) Curtiss, L. A.; Raghavachari, K.; Redfern, P. C.; Pople, J. A. Assessment of Gaussian-2 and density functional theories for the computation of enthalpies of formation. J. Chem. Phys. **1997**, 106, 1063–1079.

(25) Curtiss, L. A.; Redfern, P. C.; Raghavachari, K.; Pople, J. A. Gaussian-3X (G3X) theory: Use of improved geometries, zero-point energies, and Hartree–Fock basis sets. J. Chem. Phys. **2001**, 114, 108–117.

(26) Staroverov, V. N.; Scuseria, G. E.; Tao, J.; Perdew, J. P. Comparative assessment of a new nonempirical density functional: Molecules and hydrogen-bonded complexes. The Journal of Chemical Physics **2003**, 119, 12129–12137.

(27) Staroverov, V. N.; Scuseria, G. E.; Tao, J.; Perdew, J. P. Erratum: "Comparative assessment of a new nonempirical density functional: Molecules and hydrogen-bonded complexes" [J. Chem. Phys. 119, 12129 (2003)]. The Journal of Chemical Physics **2004**, 121, 11507–11507.

(28) Peng, H.; Yang, Z.-H.; Perdew, J. P.; Sun, J. Versatile van der Waals Density Functional Based on a Meta-Generalized Gradient Approximation. Phys. Rev. X **2016**, 6, 041005.

(29) Tran, F.; Stelzl, J.; Blaha, P. Rungs 1 to 4 of DFT Jacob's ladder: Extensive test on the lattice constant, bulk modulus, and cohesive energy of solids. J. Chem. Phys. **2016**, 144, 204120.

(30) Tran, F.; Blaha, P. Importance of the Kinetic Energy Density for Band Gap Calculations in Solids with Density Functional Theory. J. of Phys. Chem. A **2017**, 121, 3318–3325.

(31) Mejía-Rodríguez, D.; Trickey, S. B. Erratum: "Deorbitalization strategies for meta-generalized-gradient-approximation exchange-correlation functionals; Phys. Rev. A **96**, 052512 (2017)". Phys. Rev. A **2025**, 111, 029901(E).

(32) Sun, J.; Perdew, J. P.; Ruzsinszky, A. Semilocal density functional obeying a strongly tightened bound for exchange. Proc. Nat. Acad. Sci. (USA) **2015**, 112, 685–689.

(33) Kaplan, A. D.; Perdew, J. P. Laplacian-level meta-generalized gradient approximation for solid and liquid metals. Phys. Rev. Mater. **2022**, 6, 083803.

(34) Tran, F.; Kovács, P.; Kalantari, L.; Madsen, G. K. H.; Blaha, P. Orbital-free approximations to the kinetic-energy density in exchange-correlation MGGA functionals: Tests on solids. J. Chem. Phys. **2018**, 149, 144105.

(35) Perdew, J. P.; Burke, K.; Ernzerhof, M. Generalized Gradient Approximation Made Simple. Phys. Rev. Lett. **1996**, 77, 3865–3868, Erratum: *ibid.* **1997** *78* 1396.

(36) Francisco, H.; Cancio, A. C.; Trickey, S. B. Reworking the Tao–Mo exchange–correlation functional. III. Improved de-orbitalization strategy and faithful de-orbitalization. J. Phys. Chem. A **2024**, 128, 6018.

(37) Aprà, E.; Bylaska, E. J.; de Jong, W. A.; Govind, N.; Kowalski, K.; Straatsma, T. P.; Valiev, M.; van Dam, H. J. J.; Alexeev, Y.; Anchell, J. et al. NWChem: Past, present, and future. J. Chem. Phys. **2020**, 152, 184102.

(38) Weigend, F.; Ahlrichs, R. Balanced basis sets of split valence, triple zeta valence and quadruple zeta valence quality for H to Rn: Design and assessment of accuracy. Phys. Chem. Chem. Phys. **2005**, 7, 3297–3305.

(39) Kresse, G.; Joubert, D. From ultrasoft pseudopotentials to the projector augmented-wave method. Phys. Rev. B **1999**, 59, 1758–1775.

(40) Monkhorst, H. J.; Pack, J. D. Special points for Brillouin-zone integrations. Phys. Rev. B **1976**, 13, 5188–5192.

(41) Blöchl, P. E.; Jepsen, O.; Andersen, O. K. Improved tetrahedron method for Brillouin-zone integrations. Phys. Rev. B **1994**, 49, 16223–16233.

(42) Mejía-Rodríguez, D.; Trickey, S. B. Analysis of over-magnetization of elemental transition metal solids from the SCAN density functional. Phys. Rev. B **2019**, 100, 041113.

(43) Perdew, J. P.; Ruzsinszky, A.; Csonka, G. I.; Vydrov, O. A.; Scuseria, G. E.; Constantin, L. A.; Zhou, X.; Burke, K. Restoring the Density-Gradient Expansion for Exchange in Solids and Surfaces. Phys. Rev. Lett. **2008**, 100, 136406.

(44) Perdew, J. P.; Ruzsinszky, A.; Csonka, G. I.; Constantin, L. A.; Sun, J. Workhorse Semilocal Density Functional for Condensed Matter Physics and Quantum Chemistry. Phys. Rev. Lett. **2009**, 103, 026403.

(45) Lynch, B. J.; Truhlar, D. G. Small Representative Benchmarks for Thermochemical Calculations. J. Phys. Chem. A **2003**, 107, 8996–8999.

Graphical TOC Entry